International Journal of Computer Vision 45(1), 5–23, 2001

Histogram Preserving Image Transformations

EFSTATHIOS HADJIDEMETRIOU, MICHAEL D. GROSSBERG AND SHREE K. NAYAR
Department of Computer Science, Columbia University, New York, NY 10027, USA
stathis@cs.columbia.edu

Received July 19, 2000; Revised June 12, 2001; Accepted June 13, 2001

Abstract. Histograms are used to analyze and index images. They have been found experimentally to have low sensitivity to certain types of image morphisms, for example, viewpoint changes and object deformations. The precise effect of these image morphisms on the histogram, however, has not been studied. In this work we derive the complete class of local transformations that preserve or scale the magnitude of the histogram of all images. We also derive a more general class of local transformations that preserve the histogram relative to a particular image. To achieve this, the transformations are represented as solutions to families of vector fields acting on the image. The local effect of fixed points of the fields on the histograms is also analyzed. The analytical results are verified with several examples. We also discuss several applications and the significance of these transformations for histogram indexing.

Keywords: histogram preservation, Hamiltonian transformation, local transformation, weak perspective projection, paraperspective projection, histogram based recognition

1. Introduction

Histograms have been widely used to represent, analyze, and characterize images. One of their initial applications in indexing was the work of Swain and Ballard for the identification of 3D objects (Swain and Ballard, 1991). Currently, histograms are an important tool for the retrieval of images and video from visual databases (Niblack, 1993; Zhang et al., 1993; Smoliar and Wu, 1995; Bach et al., 1996). Some of the reasons for their wide applicability are that they can be computed easily and fast, they achieve significant data reduction, and they are robust to noise and local image transformations. Furthermore, in images that contain low level information, the histogram can be used to characterize the images. Images of manmade environments cannot always be classified using their histogram. Many manmade objects, however, have characteristic colors (Swain and Ballard, 1991). Further, the color properties of an object must be considered to make a recognition system complete. That is, a system should be able to discriminate between objects that are geometrically identical but have different colors.

Following the initial work of Swain and Ballard (1991) various indexing and recognition systems (Stricker and Orengo, 1995; Finlayson et al., 1996) based on histograms were developed. Several observations have been made about the sensitivity of the histogram to image transformations. More precisely, it is generally accepted that the histogram is relatively insensitive to viewpoint changes, and that it is possible to account for scale changes of its magnitude (Cohen and Guibas, 1999). More generally, several authors (Swain and Ballard, 1991; Finlayson et al., 1996) observed that histograms are insensitive even under certain object deformations.

The local and global histogram are also preserved under locally orderless transformations. One such example is error diffusion. This representation was analyzed extensively in the context of signal coding (Anastassiou, 1989). Griffin generalized this model and introduced it into computational vision as

scale-imprecision representation (Griffin, 1997). Later, Koenderink and Van Doorn formalized this representation into a locally orderless model for images (Koenderink and Doorn, 1999). Ginneken and Romeny discussed several applications of the locally orderless model (Ginneken and Romeny, 2000). These representations are the result of local and discontinuous transformations. In this work we examine the condition that local continuous transformations should satisfy to preserve the histogram.

We study the invariances of histograms with respect to transformations by describing those transformations in terms of vector fields. Vector fields are also widely used to represent images and optical flow. Primarily, they are used to model rigid and non-rigid motion. Some examples are fluid flow, deformations of textile textures, rubber deformations, and face motion (Huang, 1990). In addition, vector fields have also been used to model oriented planar textures (Kass and Witkin, 1987; Rao and Jain, 1992). Image vector fields have been expressed in terms of differential equations (Verri and Poggio, 1989; Verri et al., 1989). It has also been shown that the projection of 3D motion on the 2D image plane creates a motion field that can also be expressed in terms of differential equations. In a more general context, the effect of vector fields on their domain is represented with the integral theorems of Gauss and Stokes (Spivak, 1965; Marsden and Tromba, 1988; Arnold, 1989). The effect of vector fields on the histogram of an image, however, has not been studied to our knowledge.

The topology of continuous vector fields can be determined by the local topology around points where the field is zero, namely fixed points (Andronov et al., 1973). Therefore, the detection and characterization of such points is important (Ford et al., 1994; Giachetti and Torre, 1996). Sander and Zucker (1992) and Kass and Witkin (1987) detected fixed points using the Poincarre's winding number of the vector field (Andronov et al., 1973; Ford et al., 1994).

In this work we first discuss some general types of transformations that preserve the histograms. Then we study the effect of continuous transformations on the histograms and relate continuous transformations to continuous vector fields. In this context the domain of the images is continuous and can be measured with the Lebesgue measure (Royden, 1968). We define the histogram in terms of a density function on grayscale intensities. This density is derived from the Radon–Nicodym derivative of push-forward of area measure on the image to intensities (Royden, 1968). Using these models we derive the complete class of local image transformations, given as solutions of flow equations, that preserve the histogram or simply scale its magnitude.

In particular, we show that vector fields which preserve the histogram are divergence free and Hamiltonian (Abraham and Marsden, 1978; Arnold, 1989; Hadjidemetriou et al., 2000). We also show that fields whose divergence is constant simply scale the histogram (Hadjidemetriou et al., 2000). Further, we present more general classes of continuous transformations that preserve the histogram relative to a particular image. Finally, we analyze the effect of fixed points of the field on the histogram. The results are verified with several examples. We also discuss applications and the significance of these transformations. Thus, we completely describe the class of local continuous transformations with respect to which histogram recognition systems are insensitive.

2. General Invariance of Histograms

To study the invariance of the histogram with image transformations we note that transformations belong to two classes, namely, discontinuous and continuous. For discontinuous transformations it is obvious that rearranging different regions of the image by cutting, pasting, or reflecting can preserve the histogram. Such transformations preserve the global histogram.[1] In addition to these global transformations, individual pixels can also be rearranged. Clearly, permutations of the pixels in an image can preserve the global histogram. If these permutations are done locally, the local histograms are preserved. For example different types of halftoning and error diffusion (Ulichney, 1988; Foley et al., 1996; Anastassiou, 1989). Griffin (1997) and Koenderink and Van Doorn (1999) formalized the locally orderless image representation, similar to error diffusion. They introduced it into computational vision, and provided a mathematical model for their representation. These orderless transformations are usually modeled stochastically (Anastassiou, 1989; Ulichney, 1988).

Unlike permutations of regions and pixels, many of the transformations that arise in computer vision, such as projective transformations, optical flow, and deformations are locally continuous. That is, they are the result of continuous vector fields. In this work, we will examine histogram preserving transformations that can

be analyzed into continuous vector fields. Such transformations preserve not only the global histograms, but also the local histograms. Some simple examples are the translations and rotations. These transformations are called isometries. Furthermore, there is a more general class of exotic continuous local transformations that are not isometries, but still preserve the histogram. Such transformations, being the result of the action of continuous fields, also preserve the image topology.

3. Effect of Continuous Vector Fields on Histograms

As a preliminary step we present continuous models for the domain of the image and the histogram. These models are useful for analytical purposes. We also give an overview of the properties of continuous vector fields and the resulting transformations. Then, we discuss the effect of the vector fields on the domain of the image. Finally, we give several examples of a particular type of continuous transformations, the gradient transformations.

3.1. *Continuous Model for the Domains of the Images and the Histograms*

We represent the image by an image intensity map. The domain of the map is assumed to be spatially continuous with dimensions x and y (Spivak, 1965). This intensity map for a single color channel is $\mathcal{L} : \mathrm{D} \to \Re$, where $\mathrm{D} \subset \Re^2$ is the bounded region taken by the CCD that lies on the image plane $\Re^2$. Similarly, for a color image the intensity map is $\mathcal{L} : \mathrm{D} \to \Re^3$, where $\Re^3$ is a 3D color space, for example, RGB or HSV. Area of the image domain can be computed with the Lebesgue measure (Royden, 1968; Haaser and Sullivan, 1971). The domain of the measure can be any countable and bounded union or intersection of regions of the image domain.

The density value of a bin in the discrete histogram represents the number of pixels with values in the intensity range associated with that bin. In our case the bin densities represent image area and the histogram is a continuous density. The density value of a bin associated with intensity interval U is the push forward measure v given by: $v(\mathrm{U}) \equiv \int_{\mathcal{L}^{-1}(\mathrm{U})} dx\, dy$. This is because $\mathcal{L}^{-1}(\mathrm{U})$ is the part of the image that has intensities within the range U, that is, $\mathcal{L}^{-1}(\mathrm{U}) = \{(x, y) \mid (x, y) \in \Re^2 \text{ s.t. } \mathcal{L}(x, y) \in \mathrm{U}\}$. Therefore, measure $v(\mathrm{U})$ is a real number equal to the area of the image domain that has intensities in U. For example, if the domain U is the intensities in the interval $[a, b]$, the area in the image that has intensities in this range is given by $v([a, b]) = \int_{\mathcal{L}^{-1}([a,b])} dx\, dy$.

The derivative of $v(\mathrm{U})$ with respect to b happens to be the Radon-Nycodim derivative q of v as a measure (Royden, 1968) and gives the histogram as a continuous density. Therefore,

$$v(\mathrm{U}) \equiv \int_{\Phi^{-1}(\mathrm{U})} dx\, dy \equiv \int_{\mathrm{U}} q_\Phi\, dr \tag{1}$$

where r is a variable of intensities and $\mathrm{U} \subset \Re$ is a set of values of r. Formally:

Definition 1. A histogram is the Radon-Nikodym derivative of the push forward of Lebesgue measure via the intensity map (image).

The definition of the histogram in Eq. (1) can be extended for 3D color spaces. For example, to extend to RGB space, instead of integrating over the single grayscale dimension dr, as in Eq. (1), we should be integrating over the three color dimensions $dr_R dr_G dr_B$.

3.2. *Background on Vector Fields*

The domain of an image $\mathcal{L}$ can be morphed to give a new image $\tilde{\mathcal{L}}$. An interesting class of morphisms are the rubber deformations (Andronov et al., 1973). Such deformations can stretch the domain at one or more points, squeeze it, or locally change its shape and size. They cannot, however, tear, fold, or reflect the domain. Also, they do not create or destroy new regions. The vector fields causing rubber deformations must be one-to-one and continuous. More precisely, they must be twice differentiable, $\mathbf{C}^2$. The mapping preserves the topology of the image. It also maintain the intensity values of the regions.

This class of deformations can be expressed in terms of flow equations whose solutions (Spivak, 1965) give rise to families of tranformations. A family or path of transformations $\mathcal{T}_t$ is expressed as $\mathcal{T}_t(\vec{x}) : \mathbf{D} \to \Re^2$, where $\vec{x} = (x, y) \in \mathbf{D}$ is a point in the image domain, and $t \in \Re$ is the parameter of the transformation. We assume that t can vary continuously to give rise to a continuous incremental process of infinitesimal transformations. Transformations that arise in this manner satisfy several properties. Clearly, they are differentiable and give back the flow relations $\frac{d}{dt}\mathcal{T}_t = X$, where X is a vector field. Further, they include the identity transformation, $\mathcal{T}_0 = \mathrm{Id}$, a composition of two transformations gives a new transformation $\mathcal{T}_s \circ \mathcal{T}_t = \mathcal{T}_{s+t}$, and

they are invertible. The inverse of $\mathcal{T}_t$ is given by $\mathcal{T}_{-t}$. This is because $\frac{d}{dt}\mathcal{T}_t + \frac{d}{dt}\mathcal{T}_{-t} = X - X = 0$ is equal to zero. In other words, an image morphed by a differentiable field can be transformed to give back the original image. Transformations that satisfy these properties form a group (Rose, 1994). Some members of this groups are rotations, scalings, and other more exotic transformations we describe below.

The transformations of the images can be represented as an operation, or action (Rose, 1994), of a group of transformations of $\Re^2$ on images. An image map $\mathcal{L} : \mathbf{D} \to \Re$ as a result of the action of a transformation becomes $\tilde{\mathcal{L}} : \mathbf{D} \to \Re$. In this work we will show that to study the effect of transformations on the histogram of an image we only need to study the effect of the corresponding vector fields (Spivak, 1965).

3.3. Effect of Vector Fields on Image Domain

We would like to understand how transformations on the plane affect the domain of the image and the histogram. In general, a vector field X changes the area of an image and its histogram. To show this we break up the image into differential regions $dx\,dy$. The differential regions that flow along the streamlines of a field in general change their size and deform. This is shown in Fig. 1 where the field acting on the image increases the area around point **O**. The differential regions $dx\,dy$ that flow along the streamlines from an initial point **I** close to point **O** to a final point **F** farther from point **O** increase their size. Formally, the rate of change of area per unit area is called divergence. Also, the final size of differential regions is obtained by multiplying the initial size by the determinant of the Jacobian of the transformation, $det\frac{\partial \mathcal{T}_t(\vec{x})}{\partial \vec{x}}$.

In Fig. 1 the divergence is greater than zero. Therefore, the Jacobian is greater than one and thus, finally, the value of the bins of the histogram associated with intensities near point **O** are increased. More precisely, the histogram is given by $\int_{\mathcal{L}^{-1}(\mathrm{U})} det\frac{\partial \mathcal{T}_t(\vec{x})}{\partial \vec{x}}\,dx\,dy$, which is different than the original given by Eq. (1). On the other hand, if at point **O** of Fig. 1 the field was pointing in the opposite direction, then the area would decrease around **O**. Thus, the value of the histogram bins associated with the intensities around **O** would also decrease.

A type of vector fields that arises in many applications is the gradient field (Marsden and Tromba, 1988) of a certain function, H, given by

$$\nabla H = \frac{\partial H}{\partial x}\,\mathbf{i} + \frac{\partial H}{\partial y}\,\mathbf{j}, \tag{2}$$

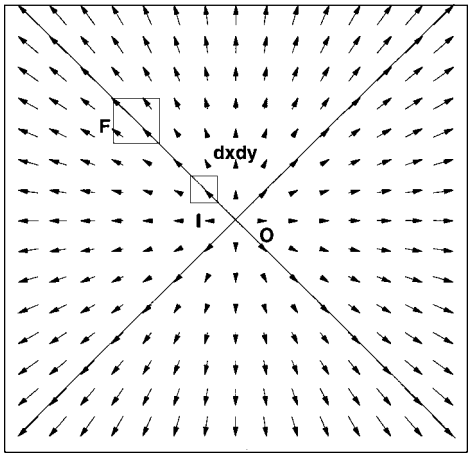

Figure 1. The area increases around the origin **O**. In other words, the field has a positive divergence around the origin. The differential areas that flow along the lines of the field from an initial point **I** close to point **O** to a final point **F** farther from point **O** grow in size.

where ∇ is the gradient, **i** is the unit vector along the x axis, and **j** is the unit vector along the y axis. The divergence of the gradient is the Laplacian. Some functions H have zero Laplacian. Thus, they do not alter the histogram, and are called harmonic. Not all functions are harmonic. Instead, their vector fields contain regions of both positive and negative divergence that, in general distort the histogram. We will show, however, that there is a class of gradient morphisms of non-zero divergence that simply scale the amplitude of the histogram. Note that gradient fields, being continuous and one-to-one, always preserve the topology of the image.

Gradient transformations can model the radial distortion of a perfectly centered lens. Radial lens distortion is modeled as (Weng et al., 1990; Swaminathan and Nayar, 1999):

$$\Delta\rho = \mathrm{k}_3\rho^3 + \mathrm{k}_5\rho^5 \tag{3}$$

where $\rho = \sqrt{x^2 + y^2}$ is the radial distance from the principal point of the image, $\Delta\rho$ is the radial distortion, and k_3 and k_5 are constants that depend on the particular lens. By integrating $\Delta\rho$ we obtain the corresponding function H_l, that is

$$H_l = \int_0^\rho \Delta\tilde{\rho}\,d\tilde{\rho} = \frac{\mathrm{k}_3}{4}\rho^4 + \frac{\mathrm{k}_5}{6}\rho^6, \tag{4}$$

where H_l is the function of the gradient field of the distortion.

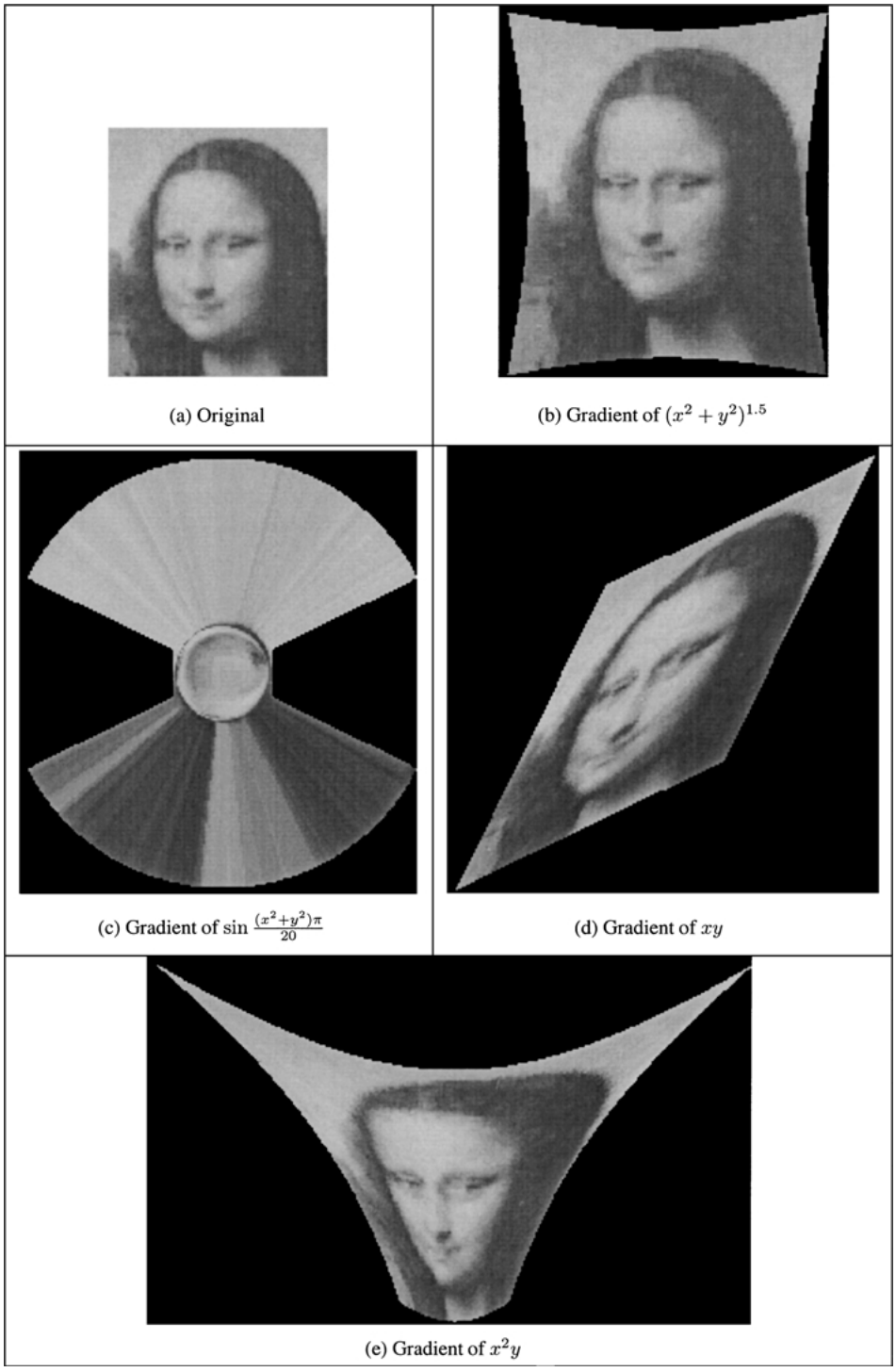

Figure 2. In (a) we show the original image and in (b)–(e) we show four gradient morphisms of this image together with the functions they correspond to. The gradient morphisms have a different histogram from the histogram of the original image. The actual distances between the histograms of these morphed images and the original image in (a) are shown in Table 2. Note that the origin of the coordinate frame is the geometrical center of the original image, the x axis is horizontal, and the y axis is vertical.

3.4. Examples of Gradient Transformations

We implemented several gradient morphisms of the test image shown in Fig. 2(a). Each one was derived from a different function H. To implement them the gradient field of the function was first computed with Eq. (2). The image was then morphed by following the tangent to the streamlines of the field with a large number of small steps. This requires resampling of the image, which was implemented using nearest neighbor. We did not implement resampling with filtering because that would introduce new intensity values not present in the original histogram. Four examples of gradient morphisms are shown in Fig. 2(b)–(e). Clearly, the topology of the image in Fig. 2(c) is different than that of Fig. 2(a). This is because the finite resolution of the image makes regions that become very small or very thin to disappear. Note that the morphed images were made rectangular by introducing a black background.

The histograms corresponding to the gradient morphisms were computed. Two of the histograms are shown in Fig. 3 where the histograms of the red, green, and blue channels are shown, respectively, from left to right. In Fig. 3(a) we show the histogram of the test image shown in Fig. 2(a). In Fig. 3(b) we show the histogram of the gradient morphism of the image shown in Fig. 2(c) that corresponds to the function $H = \sin \frac{(x^2+y^2)\pi}{20}$. For visualization purposes they were normalized with respect to their most densely populated bin. Clearly, the two histograms are different. The regions where the gradient field has divergence greater than zero increase their contribution to the histogram, whereas the regions that have negative divergence decrease their contribution. Note that the populated bins in the histograms in Fig. 3(b) are a subset of those in the histogram of the original image shown in Fig. 3(a). This is because some of the regions disappeared, but no new ones were created.

4. Image Independent Invariance of Histograms in Vector Fields

We derive the class of transformations that preserve the histogram of any image map $\mathcal{L}$. Since the histogram is

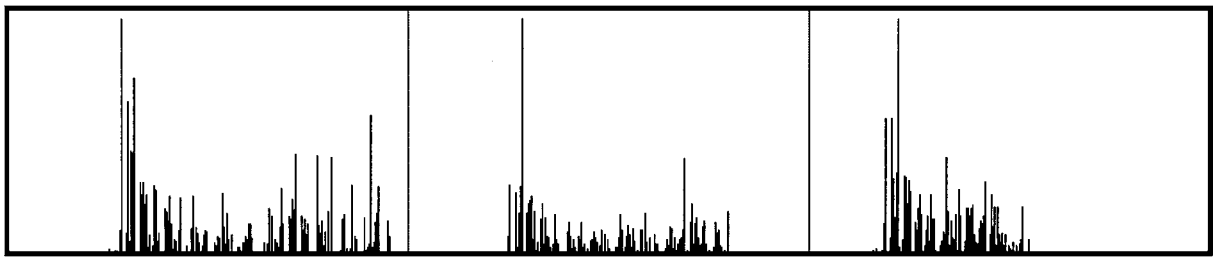

(a) Histogram of original image in Fig. 2 (a)

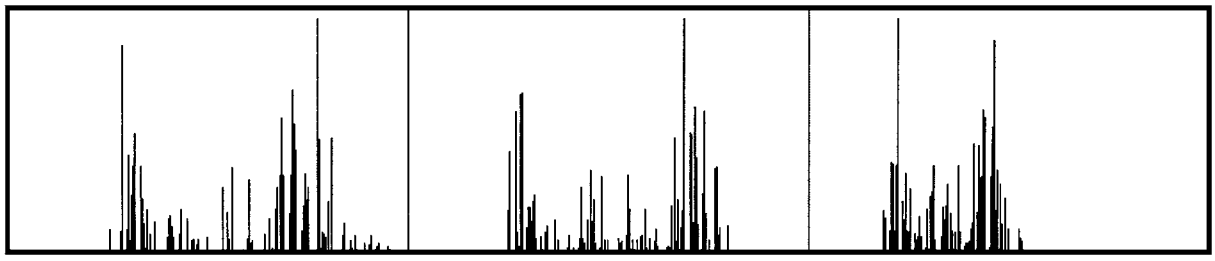

(b) Histogram of gradient morphism obtained with $\sin \frac{(x^2+y^2)\pi}{20}$

Figure 3. Histograms of two of the images in Fig. 2. From left to right are the histograms of the red, green, and blue channels, respectively. In (a) we show the histogram of the original image shown in Fig. 2(a). In (b) we show the histogram of the gradient morphism obtained with function $\sin \frac{(x^2+y^2)\pi}{20}$. The actual gradient morphism is shown in Fig. 2(c). We can see that the histogram of the gradient morphism is very different than that of the original.

given by Eq. (1), we anlayze the transformations that preserve the integral in Eq. (1) for all integration domains $\mathcal{L}^{-1}(\mathrm{U})$. For these transformations the histogram remains invariant, independent of the image.

To analyze these transformations we again break up the image into differential regions $dx\,dy$. If local size is preserved everywhere, the value of the determinant of the Jacobian of the transformation $det\frac{\partial \mathcal{T}_t(\vec{x})}{\partial \vec{x}}$ is one for all differential regions. Consequently, the histogram given by $\int_{\mathcal{L}^{-1}(\mathrm{U})} det\frac{\partial \mathcal{T}_t(\vec{x})}{\partial \vec{x}} dx\,dy$ is also preserved. On the other hand, when the histogram is preserved for all images $\mathcal{L}$, it can be shown that the determinant has to be unity everywhere. Therefore, the area is preserved. More formally:

Proposition 1. *Transformations $\mathcal{T}_t(\vec{x})$ are locally area preserving if and only if they preserve the histograms of every image $\mathcal{L}$.*

This is proved in Section A.1 of the appendix.

In general, a vector field X contains both regions of positive divergence that create area and regions of negative divergence that destroy area. If there are no regions of positive or negative divergence, however, the differential regions flow and deform but do not change their sizes. For example, in the field in Fig. 4 the differential square $dx\,dy$ moves from point **I** to point **F**, while its size remains invariant. The determinant of the Jacobian of such transformations is unity for all values of t. The rate of change of area and the divergence are zero. The rate of area change for the entire image is given by the integral of the divergence over the domain of the image. That is, $\frac{dv(t)}{dt}|_{t=t_0} = \int_{\mathrm{V}_0} divX\,dx\,dy$, where t_0 is the initial time, V_0 is the initial area, and $v(t)$ is the area at time t. If a field has zero divergence over the entire image, for all t, the total image area does not change and vice versa. That is,

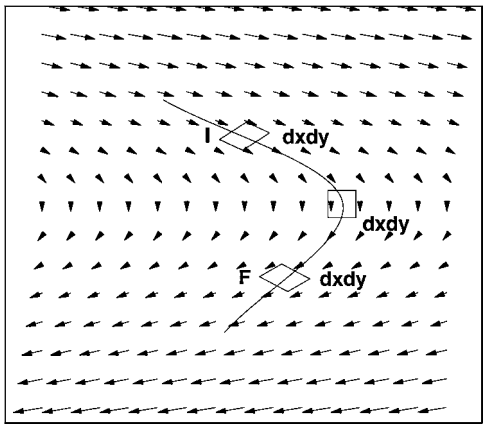

Figure 4. This field does not have regions of positive and negative divergence. Therefore, the areas of differential regions $dx\,dy$ stay the same as they move along the streamlines of the field from initial point **I** to final point **F**.

Proposition 2. *Transformations $\mathcal{T}_t$ with $\frac{d}{dt}\mathcal{T}_t = X$ are locally area preserving if and only if $divX = 0$.*

This is proved in Section A.2 of the appendix.

It is also possible to generate all vector fields that satisfy Proposition 2. To see this, take a function $H : \mathbf{D} \rightarrow \mathbf{R}$. The isovalue contours of this function are given by $H(x, y) = \mathrm{k}$, where k is a constant. The gradient of H is normal to its isovalue contours and points in the direction in which the area changes maximally. If we rotate the gradient field at every point by 90°, we obtain a new field, which is tangent to the isovalue contours of H. Flow along isovalue contours does not change the area, and the field has zero divergence. Such fields are called Hamiltonian and the flow along them is called phase flow. In 2D they are given by:

$$\Upsilon H = R_{90^\circ}(\nabla H) = \frac{\partial H}{\partial y}\mathbf{i} - \frac{\partial H}{\partial x}\mathbf{j} \qquad (5)$$

where R_{90° is the antisymmetric rotation matrix $\left[\begin{smallmatrix} 0 & 1 \\ -1 & 0 \end{smallmatrix}\right]$, and H is called the Hamiltonian function or energy function of the field. An example is Fig. 5, where Fig. 5(a) shows the function $H = \sin(xy)$ and its contours around the origin. Figure 5(b) shows the flow along the contours, that is the corresponding Hamiltonian field. Moreover, the reverse also holds. That is, if a field preserves the histogram of an image, it is Hamiltonian. More formally:

Proposition 3. *A vector field X (twice differentiable) is divergence free if and only if it is Hamiltonian.*

This is proved in Section A.3 of the appendix.

The *if and only if* Propositions 1–3 can be combined to show that the histogram preserving transformations arise as solutions to a particular family of vector fields called Hamiltonian. More precisely:

Theorem 1. *A family of transformations $\mathcal{T}_t$ which arise as the solutions to a vector field X preserve the*

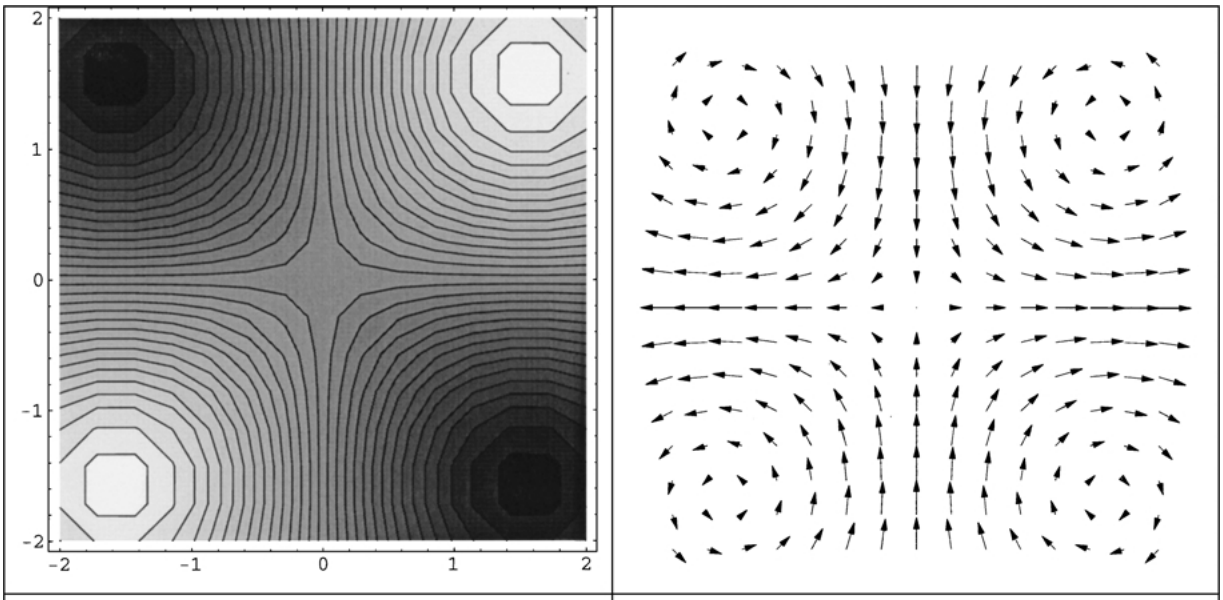

Figure 5. The image in (a) shows the energy function $H = \sin(xy)$ and its contours around the origin. Brightness is proportional to function value. The image in (b) shows the Hamiltonian field that corresponds to the flow along the isovalue contours of this function.

histograms of all images if and only if vector field X is Hamiltonian.

Proof: Propositions 1 and 2 show that the histogram is preserved if and only if the divergence of the field is zero. In turn, this combined with Proposition 3 proves the theorem. □

The determinants of the Jacobian matrices of Hamiltonian transformations, $\mathcal{T}_t(\vec{x})$, are always equal to unity.[2] This is a consequence of the area preservation property of Liouville's theorem (Arnold, 1989), which is also the *if* part of Proposition 2. Some examples of linear Hamiltonian transformations are shown in Table 1. As expected, the determinants of all the matrices in Table 1 are equal to unity.

Harmonic functions have both gradient and Hamiltonian fields which are divergence free. Therefore, the gradient field of a certain harmonic function, H, is also Hamiltonian of some other energy function $\tilde{H}$. For example, the harmonic function $H = xy$ has a gradient field which is also the Hamiltonian field of energy function $\tilde{H} = (y^2 - x^2)/2$. This field causes shearing and an example is shown in Fig. 2(d).

Table 1. The Jacobian matrices of some linear Hamiltonian transformations.

Group	Jacobian
Rotations	$\begin{pmatrix} \cos t & \sin t \\ -\sin t & \cos t \end{pmatrix}$
Shears	$\begin{pmatrix} 1 & t \\ 0 & 1 \end{pmatrix}$
Stretches	$\begin{pmatrix} t & 0 \\ 0 & 1/t \end{pmatrix}$

The determinant of the matrices is equal to one. Note that t is the parameter of the transformation.

4.1. Examples of Hamiltonian Transformations

We show several examples of linear and non-linear Hamiltonian morphisms in Fig. 6. Each one is derived from a different energy function H. These morphisms were implemented similarly to the gradient ones as described in Subsection 3.4. The only difference was that the field applied was the Hamiltonian, given by Eq. (5), instead of the gradient.

In Fig. 6(a) we show the original image, which is the same as the original image shown in Fig. 2(a). In Fig. 6(b)–(i) we show eight morphisms together with the energy functions they correspond to. The origin

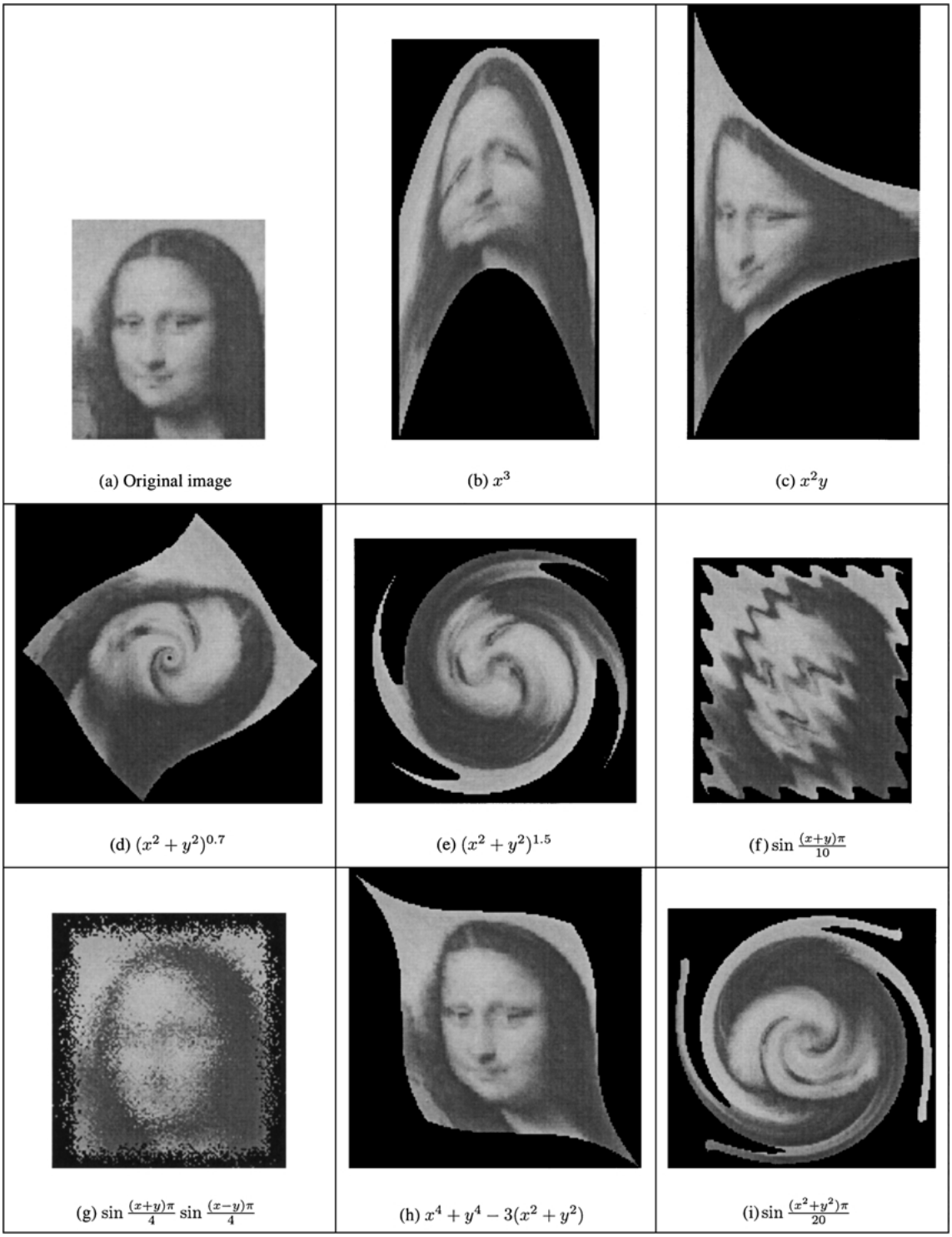

Figure 6. In (a) we show the original test image. In (b)–(i) we show eight Hamiltonian morphisms of this image and the energy functions they correspond to. All Hamiltonian morphisms have the same histogram as that of the original image, up to spatial quantization error. The actual distances between the histograms of these morphed images and the original image in (a) are shown in Table 2. Note that the origin of the coordinate frame is the geometrical center of the original image, the x axis is horizontal, and the y axis is vertical.

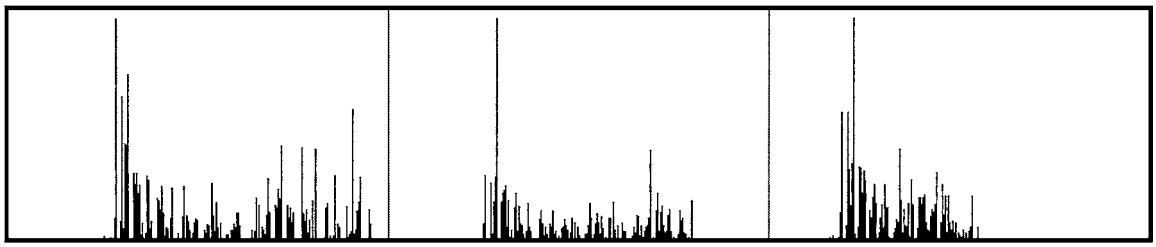

(a) Histogram of original image in Fig. 2 (a)

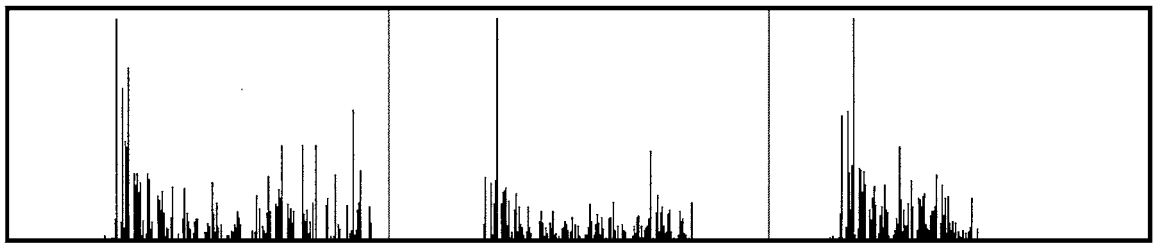

(b) Histogram of Hamiltonian morphism obtained with $(x^2.0 + y^2)^{0.7}$

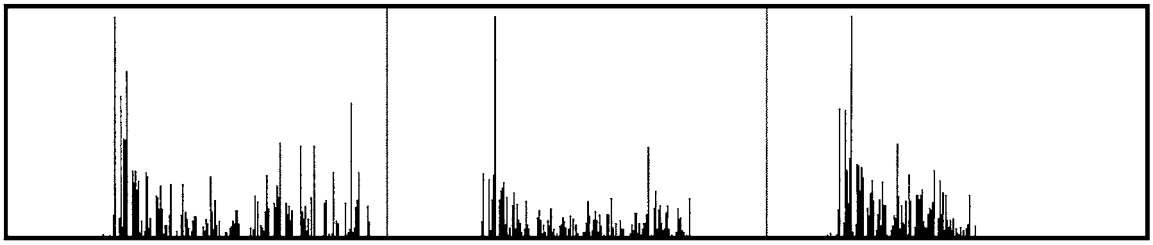

(c) Histogram of Hamiltonian morphism obtained with $x^4 + y^4 - 3(x^2 + y^2)$

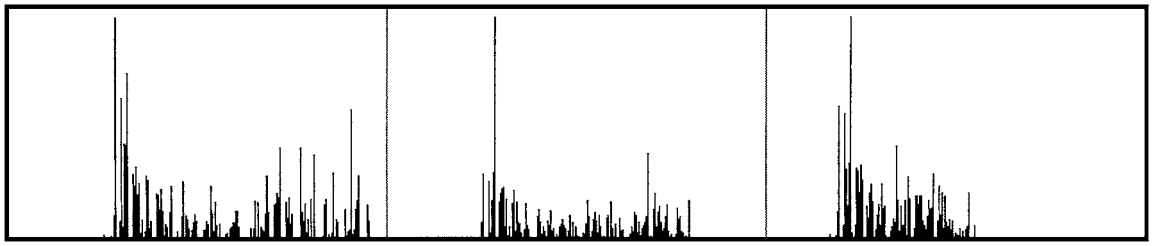

(d) Histogram of Hamiltonian morphism obtained with $\sin \frac{(x^2+y^2)\pi}{20}$

Figure 7. The histograms of several of the images in Fig. 6. From left to right are the histograms of the red, green, and blue channels of the images. In (a) we show the histogram of the original image shown in Fig. 2(a). In (b)–(d) we show the histograms of Hamiltonian morphisms. The actual Hamiltonian morphisms are shown in Fig. 6(d), (h), and (i), respectively. Clearly, the histograms of the Hamiltonians are almost the same as that of the original.

of the coordinate axes is the geometrical center of the original image. As we can see the transformed images are severely distorted.

We computed the histograms of the Hamiltonian morphisms. Some of the histograms are shown in Fig. 7; from left to right we can see the histograms of the red, green, and blue channels of the image, respectively. In Fig. 7(a) we show the histogram of the original image shown in Fig. 2(a). In Fig. 7(b)–(d) we show the histograms of the Hamiltonian morphism shown

Table 2. The effects of the Hamiltonian and gradient morphisms on the histogram.

Function	Hamiltonian	Gradient
x^3	0.488	16.763
$(x^2+y^2)^{0.7}$	1.870	121.000
(x^2+y^2)	1.302	265.641
$(x^2+y^2)^{1.5}$	2.820	42.609
$\sin\frac{(x+y)\pi}{10}$	1.003	12.182
$\left(\sin\frac{(x+y)PI}{20}\right)^2$	1.083	11.188
$\sin\frac{(x+y)\pi}{4}\sin\frac{(x-y)\pi}{4}$	6.865	13.229
xy	2.609	1.773

The histograms used were the three 1D R, G, and B histograms. The second column shows the distance of the histogram of the Hamiltonian morphism from the histogram of the original image shown in Fig. 2(a). The third column shows the distance of the histogram of the gradient morphism from the histogram of the same original image. Note that xy is a harmonic functions and that is why both its gradient and Hamiltonian fields do little. The distance is the L_1 norm of the distance between the histograms divided by the number of histogram bins (3×256).

in Fig. 6(d), (h), and (i), respectively. Clearly, the histograms of the Hamiltonian morphisms are the same as that of the original image.

We compared quantitatively the effects of the gradient and Hamiltonian morphisms of the same function applied on the same image. Actually, we compared the 1D R, G, and B histograms of the morphed images. We used the test image shown in Fig. 6(a). The second column of Table 2 shows the distance between the histogram of the original image and the histogram after the Hamiltonian morphism. The third column shows the distance between the histogram of the original image and the histogram after the gradient morphism. The distance between two histograms is the L_1 norm divided by the number of histogram bins (3×256). Clearly, the distance due to the Hamiltonian morphisms is very small. The non-zero distance is due to resampling under spatial and color quantization. On the other hand, the distance due to the gradient morphisms is much larger than that due to the Hamiltonian ones. That is, although Hamiltonian morphisms severely distort the image, the histogram of the image remains practically the same. On the other hand, these gradient transformations sometimes look like the original image, as in Fig. 2(b), but severely distort the histogram. The only exception are the morphisms of the harmonic function xy, where both its gradient and Hamiltonian fields preserve the histogram. Note that the functions were multiplied by different constant factors in each morphism to restrict the size of the morphed images.

4.2. *Histogram Scaling Transformations*

A certain class of gradient transformations simply scales the histogram. This occurs when the area change is uniformly distributed throughout the image, that is, when the divergence is spatially constant. The rate of area change is given by the divergence and the factor by which the area changes is given by the determinant of the Jacobian of the transformation. That is, Proposition 2 can be extended to state that transformations locally scale the area by a constant factor if and only if their divergence is constant. Since the histogram is linearly dependent upon the area of the image, the magnitude of the histogram is scaled by the factor the image area is scaled. Moreover, the reverse also holds. That is, if the histogram is always scaled for any image, the size of any local region in the image is scaled by the same factor. Hence, the divergence, being the rate of change of area per unit area, is also constant. In other words, we can generalize Theorem 1 to obtain:

Theorem 2. *A family of transformations $\mathcal{T}_t$ which arises as the solution to a vector field X scales the histograms of all images if and only if the vector field has constant divergence for all t. The scale factors are the determinants of the Jacobians of the transformations at any point.*

This is proved in Section A.5 of the appendix.

A simple family of transformations that satisfies Theorem 2 are the spatial image scalings, that is expansions and contractions. These transformations are given by vector fields $k_1 x\mathbf{i} + k_2 y\mathbf{j}$, where k_1, and k_2 are constants. Such vector fields are the gradients of $(\frac{k_1 x^2}{2} + \frac{k_2 y^2}{2})$ within an additive constant. The effect of such a field on the histogram is given in row 3 of Table 2. Clearly superimposing a Hamiltonian vector field on a scaling vector field does not change the effect the scaling transformation alone has on the histogram. It can also be shown that the reverse also holds. That is, if a transformation scales the histogram it is the result of the superposition of a scaling and a hamiltonian transformation. More formally:

Proposition 4. *A family of transformations $\mathcal{T}_t$ which arises as the solution to a vector field X scales the histograms of all images if and only if the vector field is the superposition of a scaling vector field given by*

$k_1 x\mathbf{i} + k_2 y\mathbf{j}$ *and an arbitrary Hamiltonian field, where* k_1, *and* k_2 *are constants.*

This is proved in Section A.5 of the appendix.

In this case the divergence is a linear map from a vector to a scalar. The null space of this map are the divergence free vector fields (Hamiltonian).

5. Applications and Significance of Hamiltonian Fields

We first study the effect of some projection models on the histogram. Clearly, perspective projection does not preserve the histogram. The perspective projection of planar surfaces whose normal is parallel to the optical axis, and rototranslations of such surfaces, however, simply scale the histograms. We will also use the two theorems presented previously to show that weak perspective projection and paraperspective projection of planar surfaces scale the histograms. Furthermore, rototranslations about any axis under these projection models also scale the histograms. We also give some more general cases that can be modeled as Hamiltonian. Finally, we discuss the significance of Hamiltonian transformations for the histogram particularly when it is used as an image feature.

5.1. Histograms under Weak Perspective Projection

Consider a planar patch, with some texture on it, in a space equipped with an $\hat{x}\hat{y}\hat{z}$ coordinate frame. The weak perspective projection of this patch is shown in Fig. 8(a). The first stage of the projection is an orthographic projection and the second is a mapping on the image plane. The orthographic projection can be done either frontally or under some arbitrary tilt ϕ. The effect of a tilt is to transform the frontal orthographic projection with an affine transformation (Basri, 1996). In this case the affine transformation is a composition of shearing and scaling. The shearing is a Hamiltonian transformation. According to Theorem 1 it does not affect the histogram. The scaling, however, does alter the histogram. In particular, according to Theorem 2, it scales it by the determinant of the Jacobian of the transformation, which is $\cos\phi$.

The second stage, that is the mapping from the projection plane to the image plane, is a uniform scaling. The determinant of its Jacobian is $\frac{f^2}{z^2}$, where f is the focal length and z is the distance of the object from the origin of the coordinate system. According to Theorem 2 this is also the scale factor of the histogram.

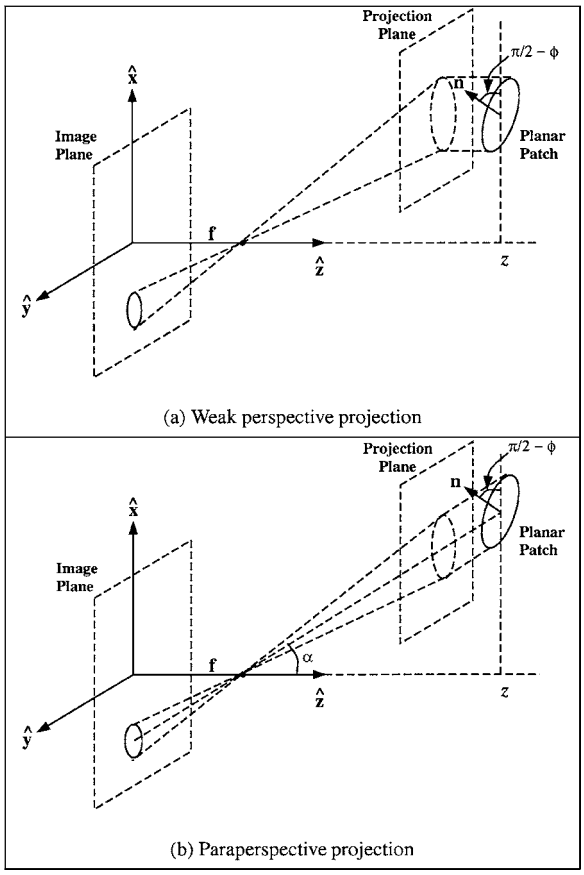

Figure 8. In (a) we can see the geometry of weak perspective projection. A planar patch is projected under a tilt angle ϕ. In (b) we show the geometry of paraperspective projection. The skew angle of the parallel projection is α, and the tilt of the object is ϕ.

The product m_w of the scaling factors of the two stages is given by

$$m_w = \frac{f^2 \cos\phi}{z^2}. \tag{6}$$

This equation gives the overall scaling of the histogram in weak perspective projection. That is, $q_{wp} = m_w q_p$, where q_p is the histogram of the frontal projection of the patch, and q_{wp} is the histogram of the patch under weak perspective projection.

5.2. Histograms under Paraperspective Projection

The paraperspective projection of a planar patch is shown in Fig. 8(b). The first stage of the projection is

a parallel projection towards the projection plane and the second stage is a mapping from the projection plane to the image plane. The parallel projection towards the projection plane has a skew angle α. Similarly to weak perspective projection, the determinant of the Jacobian of the projection transformation is proportional to the cosine of the tilt of the object. In parallel projection, however, the projection axis is skewed. Therefore, the relative tilt of the object is $(\phi - \alpha)$. Moreover, the size of the projected image increases as a result of the skew angle by a factor inversely proportional to $\cos\alpha$. That is, the determinant of the Jacobian of the parallel projection transformation is $\frac{\cos(\phi-\alpha)}{\cos\alpha}$. According to Theorem 2 the histogram is scaled by this factor.

The second stage, that is the mapping to the image plane is a uniform scaling. Similarly to weak perspective projection, this mapping scales the histogram by $\frac{f^2}{z^2}$. The overall scale factor m_p of the histogram is equal to the product of the two scale factors and is given by

$$m_p = \frac{f^2 \cos(\phi - \alpha)}{z^2 \cos\alpha}. \tag{7}$$

That is, the histogram, q_{pp} of the patch under paraperspective projection is given by $q_{pp} = m_p q_p$, where q_p is the histogram of the frontal projection of the patch. Note that paraperspective projection reduces to weak perspective projection when the angle with the optical axis α is zero.

For example, Eqs. (6) and (7) show that the change in the magnitude of the histogram of an object approaching the image plane is a scale factor.

5.3. *Discussion on Significance of Hamiltonian Transformations*

We would like to discuss the significance of Hamiltonian transformations for computational vision. In particular:

- Several authors have suggested using histograms for object recognition (Swain and Ballard, 1991; Stricker and Orengo, 1995; Finlayson et al., 1996). Furthermore, histograms are used extensively for image indexing (Niblack, 1993; Bach et al., 1996) and video retrieval (Smoliar and Wu, 1995) from visual databases. In the context of recognition it has been observed that histograms are robust to local image deformations (Swain and Ballard, 1991; Finlayson et al., 1996). The complete class of local vector fields with respect to which histogram recognition and indexing systems are insensitive is the Hamiltonian.
- Hamiltonian transformations can be used to compare recognition systems based on histograms to recognition systems based on other appearance features. For example, to compare recognition based on intesity histograms to recognition based on eigenspace (Sirovich and Kirby, 1987; Turk and Pentland, 1991; Moghaddam and Pentland, 1995; Murase and Nayar, 1995) we can investigate the sensitivity of the eigenspace representation to Hamiltonian transformations.
- The histogram is equivalent by an invertible transformation to the generalized image entropies (Tsallis, 1988; Sporring and Weickert, 1999) and the multifractal spectrum of images (Halsey et al., 1986; Sporring and Weickert, 1999). That is, Hamiltonian transformations preserve both the generalized image entropies of the image and its multifractal spectrum. In turn, both entropy (Jagersand, 1995; Wu and Barba, 1998; Sporring and Weickert, 1999; Bouzouba and Radouane, 2000) and multifractals (Vehel et al., 1992; Arneodo et al., 1999) have been used to characterize images and textures.
- In a relevant image representation the image is specified in terms of local histograms. Examples of this representation include error diffusion (Ulichney, 1988; Anastassiou, 1989), scale-imprecision space (Griffin, 1997), and locally orderless image representation (Koenderink and Doorn, 1999). In this case the local and global histograms of an image remain invariant under local discontinuous transformations. The local but continuous transformations which preserve both local and global histograms are the Hamiltonian transformations. Such transformations preserve local topology as well. An example is the transformation in Fig. 6(g).
- Several image features are based on histograms. For example, histograms have been combined with representations of connectedness of image regions to give features which combine color and spatial image information (Pass et al., 1996; Smith and Chang, 1996). We expect such features to be insensitive to Hamiltonian transformations, since Hamiltonian fields preserve the connectedness of image regions. For the same reason we expect image segmentation based on the histogram to be less sensitive to Hamiltonian transformations (Glasbey, 1993).
- In addition to the projection models discussed previously Hamiltonian transformations can model other

specific cases of distortion. For example, shearing that results from the distortion when the axes of a CCD are not orthogonal is a Hamiltonian transformation. Such transformations can also model some natural situations, for example, the flow of incompressible fluids. The morphism in Fig. 6(f) shows ripples or sinusoidal vibrations along a surface, and the morphism in Fig. 6(d) resembles a whirlpool.

6. Image Dependent Invariance of Histograms for Vector Fields

The Hamiltonian transformations that satisfy Theorem 1 preserve the histogram of all images $\mathcal{L}$. For a particular image $\mathcal{L}$, however, there is a more general class of transformations that preserve its histogram. These transformations preserve the histogram for only a particular image.

In all cases, both image dependent and image independent, the histogram is preserved when the following equation is satisfied:

$$\begin{aligned}\tilde{v}(\mathrm{U}, t) &= \int_{\mathcal{L}^{-1}(\mathrm{U})} det\, \frac{\partial \mathcal{T}_t(\vec{x})}{\partial \vec{x}}\, dx\, dy \\ &= \int_{\mathcal{L}^{-1}(\mathrm{U})} dx\, dy \end{aligned} \tag{8}$$

where $\tilde{v}(\mathrm{U}, t)$ is the histogram value in intensity bin U as a function of parameter t. In the image independent case, we showed that Eq. (8) holds when the size of the image regions within or between all isovalue contours containing regions within intensity intervals U remain constant. That is, we assumed that the value of the Jacobian for every differential region is equal to one. This condition guarantees that the histogram is preserved. It is, however, overly restrictive. More generally, it is sufficient for a continuous field to preserve the total size of the regions in an image inside isovalue contours. That is, instead of forcing the divergence to be zero everywhere within all isovalue contours, we just require that the average value of the divergence be zero within the isovalue contours. Since the histogram is computed over the entire image domain, the histogram is still preserved.

The change of the size of the region within an isovalue contour as a result of a transformation depends on the divergence of the field over that region. More precisely, the rate of change of the size of a region is given by the integral of the divergence over that region. Therefore, if the integral of the divergence within all isovalue contours is zero, the rate of change of area is also zero and the contribution of all intensities to the histogram does not change. This condition can be expressed both in terms of the divergence over regions and in terms of line integrals of vector fields along the contours of the regions. The relation between the two is given by Gauss's theorem (Marsden and Tromba, 1988). More precisely, the surface integral of the divergence of a field over a certain region is equal to the line integral of the field along the border of that region. Therefore, the condition that the integral of the divergence over a certain region be zero is the same as the condition that the line integral along the borders of the region be zero. That is:

Proposition 5. *The histogram of a particular image $\mathcal{L}$ is preserved as a result of a transformation $\mathcal{T}$, and Eq.* (8) *is satisfied if*:

$$\oint_c X = 0, \forall C \tag{9}$$

where C is an arbitrary isovalue contour of the image.

This is proved in Section A.4 of the appendix.

This proposition implies that for a given image there is a class of fields that preserve its histogram, and, vice versa, for a given field there is a class of images whose histograms are preserved under the action of the field.[3]

This proposition can model the rotation and translation of rigid bodies in front of a uniform background. Such motion appears to be the result of cut and paste. It can also occur, however, when within the windows of motion the field is non-zero and continuous, and outside the windows the field is zero. The windows of motion are the regions in which the motion occurs. Image dependent transformations[4] can also model some cases of lens distortions. Such an example would be images that consist of radially symmetric patterns scaled by radial lens distortion. In general, the transformations described in this section are significant for most of the reasons for which the Hamiltonian transformation are significant, as discussed in Subsection 5.3.

7. Local Topology of Vector Fields and Histograms

The topology of vector fields can be determined by the topology around fixed points in the fields (Andronov

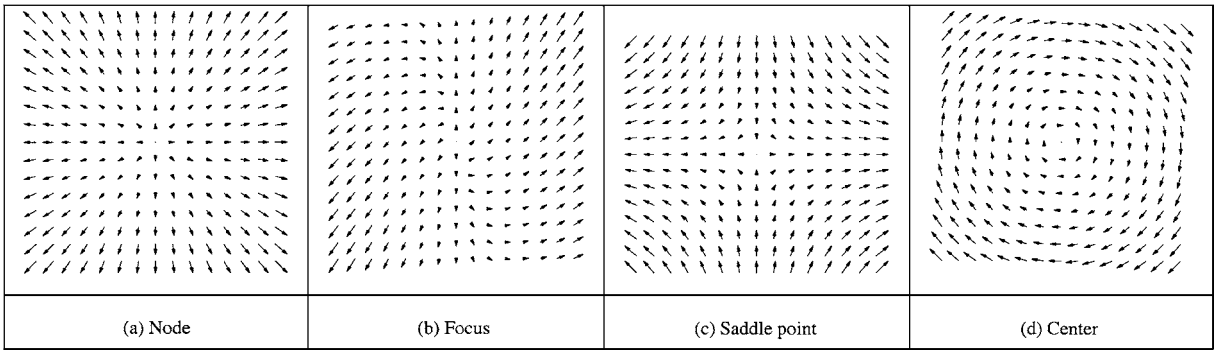

Figure 9. Possible topologies around fixed points of a field. In (a) the fixed point is called node. In (b) the topology is spiral and the fixed point is called a focus. In (a) and (b) the orientation of the paths is away from the fixed points. In (c) we can see a saddle point. Finally, in (d) the fixed point is called a center.

et al., 1973). That is, points where the field is zero. In gradient and Hamiltonian fields the fixed points are the critical points of the energy function. The images in Fig. 6 contain several fixed points, for example, along the vertical line $x = 0$ in Fig. 6(b), and the central point of the images in Figs. 6(d)–(e).

There are four different kinds of fixed points (Andronov et al., 1973). The first kind is shown in Fig. 9(a) and is called a *node*. In this case the integral curves are lines arranged radially around the fixed point with one end on the fixed point (star-shaped). The second kind is shown in Fig. 9(b) and is called a *focus*. In this case the integral curves still have one end on the fixed point. They form, however, spirals around it. In these two cases the fixed points can be sinks or sources depending on the direction of the integral curves. The third kind is shown in Fig. 9(c) and is called a saddle point. Two ridges meet to create four lines of fixed points. Finally, the fourth kind is shown in Fig. 9(d) and is called a *center*. The integral curves form closed paths around the fixed point.[5] For example the circles $\frac{(x^2+y^2)}{20} = n$ where $n = 1, 2, \ldots$ shown in Fig. 2(c).

Fixed points can be detected and classified using the Poincarre's winding number. This was introduced in image processing by Sander and Zucker (1992) and by Kass and Witkin (1987).

The topological structure around a fixed point has a direct effect on the histogram. Fixed points of type (a), and type (b) are sources or sinks that locally distort the histogram. For example, the center of the image, or principal point, in radial lens distortion (Weng et al., 1990; Swaminathan and Nayar, 1999) is a fixed point of type (a). When the field is linear, however, the histogram is simply scaled. On the other hand, fixed points of type (c) and type (d) preserve the local histograms. Such an example is shown in Fig. 2(d) where there is a saddle point in the middle of the image.

Hamiltonian fields, which preserve the histogram for all images, must only have fixed points of type (c) and (d). The converse does not hold. That is, a field with fixed points of type (c) and (d) is not necessarily Hamiltonian. Transformations that preserve the histogram relative to a particular image can have fixed points of any type, including sources, sinks, and spirals. This is because the effects of sources and sinks can cancel out to preserve the histogram.

8. Summary and Future Work

In general, histogram preserving transformations can be either orderless or the result of the action of continuous fields. In this work we examined histogram preserving transformations that are the result of the action of continuous fields. For this purpose, we examined the effect on histograms of transformations that result from the action of general continuous fields. To analyze their effect we assumed that the image was spatially continuous and used the Lebesgue measure to compute its area. Then, a measure was defined on the range of the image map that gave its histogram. Using these models we derived the complete classes of local image transformations that preserve the histogram of all images up to a scale factor of their magnitude.

We showed that local transformations that can be expressed as solutions to flow equations preserve the histogram of all images if and only if the divergence of the vector fields is zero and that such fields are Hamiltonian. Furthermore, the histogram of any image

is scaled if and only if the divergence of the fields is constant everywhere. We also examined a more general condition that transformations should satisfy in order to preserve the histogram of a particular image. We then gave several examples of deformations that result from Hamiltonian fields. The images were completely deformed but their histograms remained the same. We completed the analysis with a discussion of the relation between the nature of the fixed points of a field and the changes on local histograms.

We also discussed some applications as well as the significance of these fields. They can model weak perspective projection, paraperspective projection, and image shearing. More generally, they can model the flow of incompressible fluids and all continuous transformations with respect to which histogram recognition systems are insensitive. We also showed that they can achieve an effect similar to that of error diffusion.

This work could be extended in serveral ways. It could be extended to volume preserving transformations for 3D data. The sensitivity of the histogram with respect to non-Hamiltonian transformations could also be studied. Furthermore, other image features may also have classes of transformations with respect to which they are invariant or have a small sensitivity. Such features can be histograms of images resulting from derivative filtering (Schiele and Crowley, 2000).

Appendix

A.1. Proof of Proposition 1

Proposition 1 states that transformations $\mathcal{T}_t(\vec{x})$ are locally area preserving if and only if they preserve the histograms of every image $\mathcal{L}$.

Proof: The histogram of image $\mathcal{L}$ transformed by $\mathcal{T}_t$ is given by:

$$\tilde{v}(\mathrm{U}, t) = \int_{\mathcal{L}^{-1}(\mathrm{U})} det \frac{\partial \mathcal{T}_t(\vec{x})}{\partial \vec{x}}\, dx\, dy \tag{10}$$

where $\tilde{v}(\mathrm{U}, t)$ is the histogram value for intensity bin U as a function of parameter t, and $det\frac{\partial \mathcal{T}_t(\vec{x})}{\partial \vec{x}}$ is the determinant of the Jacobian of the transformation. Since the transformation is locally area preserving, the determinant is equal to unity (Arnold, 1989); that is,

$$det \frac{\mathcal{T}_t(\vec{x})}{\partial \vec{x}}\, dx\, dy = dx\, dy. \tag{11}$$

Therefore, the histogram of the transformed image becomes

$$\tilde{v}(\mathrm{U}, t) = \int_{\mathcal{L}^{-1}(\mathrm{U})} dx\, dy. \tag{12}$$

This histogram is the same as that of the original image, hence, the histogram is preserved. Conversely, take some set $V \subset D$ of the image domain. We define an indicator image function $\mathcal{L}$ such that

$$\mathcal{L}_I(\vec{x}) = \begin{cases} 1 & \text{if and only if } \vec{x} \in \mathrm{V}, \\ 0 & \text{otherwise.} \end{cases} \tag{13}$$

Since the histogram of $\mathcal{L}_I$ is preserved, we have: $\int_{\mathrm{V}_0} dx\, dy = \int_{\mathrm{V}_1} dx\, dy, \forall t$, where V_1 is V_0 after $\mathcal{T}_t$ is applied. Region V_0 can be any local area, hence, $\mathcal{T}_t$ are locally area preserving $\forall t$. □

A.2. Proof of Proposition 2

Proposition 2 states that transformations $\mathcal{T}_t$ with $\frac{d}{dt}\mathcal{T}_t = X$ are loclly area preserving if and only if $divX = 0$.

Proof: The *if* part of this Proposition is Liouville's theorem (Abraham and Marsden, 1978; Arnold, 1989). Take some set $\mathrm{V}_0 \subset \mathbf{D}$ of the image domain corresponding to intensity interval U. After the application of transformation $\mathcal{T}_t$ the area of V_0 becomes:

$$\tilde{v}(\mathrm{U}, t) = \int_{\mathrm{V}_0} det \frac{\partial \mathcal{T}_t(\vec{x})}{\partial \vec{x}}\, dx\, dy \tag{14}$$

Take $\tilde{t} = t - t_0$, When $\tilde{t} = t - t_0$ is close to zero the Jacobian can be expanded as in Liouville's theorem in Arnold (1989) to get

$$\tilde{v}(\mathrm{U}, \tilde{t}) = \int_{\mathrm{V}_0} (1 + \tilde{t}\, divX + O(\tilde{t}^2))\, dx\, dy \tag{15}$$

where div is the divergence (Marsden and Tromba, 1988). This equation can be differentiated $\frac{d\tilde{v}(\mathrm{U},\tilde{t})}{d\tilde{t}} \mid_{\tilde{t}=0} = \frac{d\tilde{v}(\mathrm{U},t)}{dt} \mid_{t=t_0}$ to give:

$$\left.\frac{d\tilde{v}(\mathrm{U}, t)}{dt}\right|_{t=t_0} = \int_{\mathrm{V}_0} divX\, dx\, dy. \tag{16}$$

Hence, if $divX = 0$ then $\tilde{v}(\mathrm{U}, t) = \mathrm{V}_0 \forall t$. That is, the transformations are locally area preserving. Conversely, if the family is locally area preserving we have $\frac{d\tilde{v}(\mathrm{U},t)}{dt} = 0$ for all t. Moreover, this holds for all V_0

given by an indicator image as in Eq. (13). Therefore, $divX = 0$. □

A.3. Proof of Proposition 3

Proposition 3 states that a vector field X (twice differentiable) is divergence free if and only if it is Hamiltonian.

Proof: The divergence of the Hamiltonian is given by:

$$\begin{aligned} div(\Upsilon H) &= div\left(\frac{\partial H}{\partial y} - \frac{\partial H}{\partial x}\right) \\ &= \frac{\partial^2 H}{\partial x \partial y} - \frac{\partial^2 H}{\partial y \partial x} = 0 \end{aligned}$$

It follows from the equality of mixed partial derivatives that the Hamiltonian fields are divergence free. Moreover, the reverse also holds. Take a vector field $X = f\mathbf{i} + g\mathbf{j}$ which has $divX = \frac{\partial f}{\partial x} + \frac{\partial g}{\partial y} = 0$. Because of the definition of the Hamiltonian field X in Eq. (5), we first define $f = \frac{\partial H}{\partial y}$. This gives $H(x, y) = \int_0^y f(x, \tilde{y})\, d\tilde{y}$. If we also show that $-\frac{\partial H}{\partial x} = g$, H is the Hamiltonian of the field. Indeed,

$$\begin{aligned} -\frac{\partial H}{\partial x} &= -\int^y \frac{\partial f(x, \tilde{y})}{\partial x}\, d\tilde{y} \\ &\overset{1}{=} \int^y \frac{\partial g(x, \tilde{y})}{\partial \tilde{y}}\, d\tilde{y} \overset{2}{=} g \end{aligned}$$

where 1 holds because $divX = 0$, and 2 follows from the fundamental theorem of calculus. □

A.4. Proof of Proposition 5

This Proposition states that the histogram of a particular image $\mathcal{L}$ is preserved as a result of a transformation $\mathcal{T}_t$, that is Eq. (8) is satisfied, if and only if:

$$\oint_c X = 0, \forall C \tag{17}$$

where C is an isovalue contour of the image.

Proof: We can apply Gauss's law (Marsden and Tromba, 1988) in Eq. (17) to obtain

$$\oint_c X = \int_{\mathrm{V}} div\mathrm{X}_t = 0 \tag{18}$$

where $\partial V = C$ is an isovalue contour curve that is the boundary of region V that can also be the union of many disconnected regions. This equation holds for all t. It can be substituted into Eq. (16) to show that the rate of change of the area is zero for all t. That is, the size of regions V is preserved. In turn, Eq. (1) relates the size of the regions to the histogram. It shows that when the size of the regions is preserved, the histogram is also preserved. □

This theorem could be generalized to cases where the histogram of regions is scaled. This occurs when the RHS of the integral of Eq. (18) is constant instead of zero.

A.5. Proof of Theorem 2

Theorem 2 states that a family of transformations $\mathcal{T}_t$, which arises as the solution to a vector field X, scales the histograms of *all* images if and only if the vector field has constant divergence for all t. The scale factors are the determinants of the Jacobians of the transformations at any point.

Proof: We can generalize Proposition 1 to get that: *Transformations $\mathcal{T}_t$ locally scale the area if and only if they scale the histogram of every image $\mathcal{L}$.* To see that this is possible consider the fact that if the histogram is scaled by a constant for any image $\mathcal{L}$, it is also scaled for any indicator image given by Eq. (13). Since the indicator image can represent any local region, all local areas are scaled by the same factor. The reverse can be shown similarly. We can also generalize Proposition 2 to get that: *Transformations $\mathcal{T}_t$ with $\frac{d}{dt}\mathcal{T}_t = X$ locally scale the area if and only if div X is constant*. The rate of change of area is proportional to the divergence. Hence, if the divergence is constant, then the rate of change of area is constant. That is, the area is scaled. In turn, this implies that the rate of change of area and the divergence are constant. The generalizations of Propositions 1 and 2 are both *if and only if*. Therefore, they can be combined to give the theorem.

Further, when the divergence is constant for all t any higher order derivatives of the function H must be zero, since they are derivatives of constants. In turn, higher order terms in the expansion of $det\, \frac{\partial \mathcal{T}_t(\vec{x})}{\partial \vec{x}}$, as shown in the integrand of Eq. 15, must also be zero. In turn, this implies that the determinant of the Jacobian of the transformation is also constant and can be factored out of the integral in Eq. (10) to give the scaling factor of the area. □

Proposition 4 states that a family of transformation $\mathcal{T}_t$ which arises as the solution to a vector field X scales the histograms of all images if and only if the vector field is the superposition of a scaling field given by $(\mathrm{k}_1 x\mathbf{i} + \mathrm{k}_2 y\mathbf{j})$ and an arbitrary Hamiltonian field, where k_1, and k_2 are constants.

Proof: In this case the divergence is a linear map from a vector to a scalar. The null space of this map are the divergence free vector fields (Hamiltonian). To see this consider a vector field $X = \mathrm{k}_1 x\mathbf{i} + \mathrm{k}_2 y\mathbf{j}$, where k_1 and k_2 are constants. This field has divergence $\mathrm{k}_{tot} = \mathrm{k}_1 + \mathrm{k}_2$ and is the gradient of $(\frac{\mathrm{k}_1 x^2}{2} + \frac{\mathrm{k}_2 y^2}{2})$ within an additive constant. Suppose Y were some other vector field with the same constant divergence k_{tot}. Since divergence is linear, the vector field $Z = Y - X$, where $X = \mathrm{k}_1 x\mathbf{i} + \mathrm{k}_2 y\mathbf{j}$, must be divergence free. Hence, as shown in Proposition 3, Z must be Hamiltonian. Thus, every vector field Y that has constant divergence also has the form $Y = X + Z$, where Z is a Hamiltonian field, and X is as above. □

Notes

1. Different scales of a fractal image can also have the same global histogram.
2. The product of two Hamiltonian transformations is another Hamiltonian transformation, which still has Jacobian with unit determinant. The product of two Hamiltonian transformations with energy functions H_1 and H_2, however, commute if and only if the Poisson bracket of the two functions, (H_1, H_2), is locally constant (Arnold, 1989).
3. If the RHS of Eq. (9) were constant, the histogram would simply be scaled.
4. Image dependent histogram preserving transformations do not necessarily commute with other fields, even Hamiltonian ones. Two vector fields commute if and only if their Lie brackets commute.
5. In some cases the integral curves can also form *spirals* that have one end on the fixed point. The fixed point is then called *centrofocus.*

References

Abraham, R. and Marsden, J.E. 1978. *Foundations of Mechanics*. Benjamin/Cummings: New York.

Anastassiou, D. 1989. Error diffusion coding for A/D conversion. *IEEE Transactions on Circuits and Systems*, 36(9):1175–1186.

Andronov, A.A., Leontovich, E.A., Gordon, I.I., and Maier, A.G. 1973. *Qualitative Theory of Second-Order Dynamic Systems*. John Wiley and Sons: New York.

Arneodo, A., Decoster, N., and Roux, S.G. 1999. Intermittency, log-normal statistics, and multifractal cascade process in high-resolution satellite images of cloud structure. *Physical Review Letters*, 83(6):1255–1258.

Arnold, V.I. 1989. *Mathematical Methods of Classical Mechanics*. Springer-Verlag: New York.

Bach, J.R., Fuler, C., Gupta, A., Hampapur, A., Horowitz, B., Humphrey, R., Jain, R., and Shu, C. 1996. The Virage image search engine: An open framework for image management. In *SPIE Conference on Storage and Retrieval for Image and Video Databases IV*, March 1996. Vol. 2670, pp. 76–87.

Basri, R. 1996. Paraperspective=Affine. *International Journal of Computer Vision*, 19(2):169–179.

Bouzouba, K. and Radouane, L. 2000. Image identification and estimation using the maximum entropy principle. *Pattern Recognition Letters*, 21:691–700.

Cohen, S. and Guibas, L. 1999. The earth mover's distance under transformation sets. In *Proc. of the 7th International Conference on Computer Vision*, Vol. 2, Kerkyra, Greece. Sept. 1999, pp. 1076–1083.

Finlayson, G.D., Chatterjee, S.S., and Funt, B.V. 1996. Color angular indexing. In *Proc. of the 4th European Conference in Computer Vision*, Vol. 2, Berlin, Germany, 1996, pp. 16–27.

Foley, J.D., van Dam, A., Feiner, S.K., and Huqhes, J.F. 1996. *Computer Graphics Principles and Practice*. Addison Wesley: Reading, MA.

Ford, R.M., Strickland, R.N., and Thomas, B.A. 1994. Image models for 2-D flow visualization and compression. *CVGIP: Graphical Models and Image Processing*, 56(1):75–93.

Giachetti, A. and Torre, V. 1996. The use of optical flow for the analysis of non-rigid motions. *International Journal of Computer Vision*, 18(3):255–279.

Ginneken, B.V. and Romeny, B.M.H. 2000. Applications of locally orderless images. *Journal of Visual Communication and image Representation*, 11:196–208.

Glasbey, C.A. 1993. An analysis of histogram-based thresholding algorithms. *Computer Vision, Graphics, and Image Processing*, 55(6):532–537.

Griffin, L.D. 1997. Scale-imprecision space. *Image and Vision Computing*, 15:369–398.

Haaser, N.B. and Sullivan, J.A. 1971. *Real Analysis*. Dover Publications: New York.

Hadjidemetriou, E., Grossberg, M.D., and Nayar, S.K. 2000. Histogram preserving image transformations. In *Proc. of the IEEE Conference on Computer Vision and Pattern Recognition*, Vol. 1, South Carolina, June 2000, pp. 410–416.

Halsey, T.C., Jensen, M.H., Kadanoff, L.P., Procaccia, I., and Shraiman, B.I. 1986. Fractal measures and their singularities: The characterization of strange sets. *Physical Review A*, 33(2):1141–1151.

Huang, T.S. 1990. Modeling, analysis and visualization of nonrigid object motion. In *Proc. of IEEE International Conference of Pattern Recognition*, June 1990, pp. 361–364.

Jagersand, M. 1995. Saliency maps and attention selection in scale and spatial coordinates: An information theoretic approach. In *Proc. of the 5th IEEE International Conference on Computer Vision*, June 1995, pp. 195–202.

Kass, M. and Witkin, A. 1987. Analyzing oriented patterns.*Computer Vision Graphics and Image Processing*, 37:362–385.

Koenderink, J.J. and Van Doorn, A.J. 1999. The structure of locally orderless images. *International Journal of Computer Vision*, 31(2/3):159–168.

Marsden, J.E. and Tromba, A.J. 1988. *Vector Calculus*. W.H. Freeman and Company: New York.

Moghaddam, B. and Pentland, A. 1995. Maximum likelihood detection of faces and hands. In *International Workshop on automatic Face-and-Gesture Recognition*, 1995, pp. 122–128.

Murase, H. and Nayar, S. 1995. Visual learning and recognition of 3D objects from appearance. *International Journal of Computer Vision*, 14:5–24.

Niblack, W. 1993. The QBIC project: Querying images by content using color, texture, and shape. In *SPIE Conference on Storage and Retrieval for Image and Video Databases*, April 1993, Vol. 1908, pp. 173–187.

Pass, G., Zabih, R., and Miller, J. 1996. Comparing images using color coherence vectors. In *Proc. of ACM Multimedia*, 1996, pp. 65–73.

Rao, A.R. and Jain, R.C. 1992. Computer flow field analysis: Oriented texture fields. *IEEE Transactions on Pattern Analysis and Machine Intelligence*, 14(7):693–706.

Rose, J.S. 1994. *A Course on Group Theory*. Dover: New York.

Royden, H.L. 1968. *Real Analysis*. MacMillan: New York.

Sander, P.T. and Zucker, S.W. 1992. Singularities of principal direction fields from 3-D images. *IEEE Transactions on Pattern Analysis and Machine Intelligence*, 14(3):309–317.

Schiele, B. and Crowley, J.L. 2000. Recognition without correspondence using multidimensional receptive field histograms. *International Journal of Computer Vision*, 36(1):31–50.

Sirovich, L. and Kirby, M. 1987. Low-dimensional procedure for the characterization of human faces. *Journal of the Optical Society of America*, 4(3):519–524.

Smith, J. and Chang, S.F. 1996. Tools and techniques for color image retrieval. In *Proc. of SPIE*, Feb.1996, Vol. 2670, pp. 1630–1639.

Spivak, M. 1965. *Calculus on Manifolds*. Benjamin/Cummings: New York.

Sporring, J. and Weickert, J. 1999. Information measures in scale-spaces. *IEEE Transactions on Information Theory*, 45(3):1051–1058.

Stricker, M. and Orengo, M. 1995. Similarity of color images. In *Proc. of SPIE Conference on Storage and Retrieval for Image and Video Databases III*, Feb. 1995, Vol. 2420, pp. 381–392.

Swain, M.J. and Ballard, D.H. 1991. Color indexing. *International Journal of Computer Vision*, 7(1):11–32.

Swaminathan, R. and Nayar, S.K. 1999. Non-metric calibration of wide angle lenses and polycameras. In *Proc. of the IEEE Conference on Computer Vision and Pattern Recognition*, 1999, Vol. II, pp. 413–419.

Tsallis, C. 1988. Possible generalization of Boltzmann-Gibbs statistics. *Journal of Statistical Physics*, 52(1/2):479–487.

Turk, M. and Pentland, A. 1991. Eigenfaces for recognition. *Cognitive Neuroscience*, 3(1):71–86.

Ulichney, R.A. 1988. Dithering with blue noise. *Proceedings of the IEEE*, 76:56–79.

Vehel, J.L., Mignot, P., and Berroir, J.P. 1992. Multifractals, texture, and image analysis. In *Proc. of the IEEE Conference on Computer Vision and Pattern Recognition*, Champaign, Illinois, June 1992, pp. 661–664.

Verri, A., Girosi, F., and Torre, V. 1989. Mathematical properties of the two-dimensional motion field: From singular points to motion parameters. *Journal of the Optical Society of America A*, 6(5):698–712.

Verri, A. and Poggio, T. 1989. Motion field and optical flow: Qualitative properties. *IEEE Transactions on Pattern Analysis and Machine Intelligence*, 11(5):490–497.

Weng, J., Cohen, P., and Herniou, M. 1990. Calibration of stereo cameras using a non-linear distortion model. In *Proc. of the IEEE Conference on Computer Vision and Pattern Recognition*, 1990, Vol. I, pp. 246–253.

Wu, H.S. and Barba, J. 1998. Minimum entropy restoration of star field images. *IEEE Transactions on Systems, Man, and Cybernetics-Part B*, 28(2):227–231.

Zhang, H.J., Kankanhali, A., and Smoliar. S.W. 1993. Automatic partitionang of full-motion video. *Multimedia Systems*, 1:10–28.

Zhang, H.J., Low, C.Y., Smoliar W., and Wu, J.H. 1995. Video parsing, retrieval and browsing: An integrated and content-based solution. *ACM Multimedia*, pp. 15–24.